ELSEVIER

Constraints on the age and halogen composition of mantle fluids in Siberian coated diamonds

R. Burgess [a,*], E. Layzelle [a], G. Turner [a], J.W. Harris [b]

[a] *Department of Earth Sciences, University of Manchester, Oxford Rd, Manchester M13 9PL, UK*
[b] *Division of Earth Sciences, University of Glasgow, Glasgow G12 8QQ, UK*

Abstract

Extension of the Ar–Ar stepped heating technique has been used to characterise the Ar, halogen (Cl, Br, I), Ca and K components in seven coated diamonds from the Aikhal kimberlite, Siberia. At least three components have been identified with different Ar isotope compositions. The major component is characterised by high $^{40}Ar/^{36}Ar > 11\,000$ and constant $^{40}Ar*/Cl$ ($527 \pm 22 \times 10^{-6}$), Br/Cl ($1.74 \pm 0.18 \times 10^{-3}$) and I/Cl ($22.0 \pm 3.4 \times 10^{-6}$) indicative of a mantle fluid phase. This component is widespread in coated diamonds having been previously reported in samples from Africa and Canada. Estimates of halogen abundances in the sub-continental mantle, based on data from African and Siberian coated diamonds, are 3 ppm Cl, 11 ppb Br and 0.4 ppb I. These low abundances, which are in good agreement with values derived for the depleted asthenospheric mantle derived from MORB data, imply that the upper mantle is $> 90\%$ degassed of its halogens. A second Ar component in coated stones is most simply understood by in situ decay of ^{40}K and is consistent with the coat-forming event occurring close to the time of host kimberlite eruption 350–380 Ma ago. A third Ar component has a low $^{40}Ar/^{36}Ar$ ratio (~ 300), is unassociated with release of K or halogens, and is most likely to be atmospheric blank. © 2002 Elsevier Science B.V. All rights reserved.

Keywords: diamond; halogens; fluid inclusions; geochronology; argon

1. Introduction

Diamond is able to preserve crystalline and fluid syngenetic inclusions over long geological intervals. Thus studies of diamond enable examination of the chemical and isotopic composition that existed at the time of diamond growth. Since diamonds have formed at various periods through-

out Earth history and are up to 3 Ga old, their study also holds the potential of obtaining 'fossil' isotopic and chemical signatures of the ancient mantle. Formation of diamonds in cratonic keels means they sample regions of the mantle that are distinct from those of oceanic basalts, and are also those areas most likely to have been isolated from convection and homogenisation since continent formation during the Archean [1].

'Coated' diamond is composed of a clear octahedral core surrounded by a turbid fibrous overgrowth or 'coat', containing abundant sub-micrometre volatile-rich fluid inclusions [2]. The

* Corresponding author. Fax: +44-161-275-3947.
E-mail address: ray.burgess@man.ac.uk (R. Burgess).

diamond and inclusions have an isotopic signature very similar to that of mid-ocean ridge basalt (MORB) upper mantle ($\delta^{13}C = -4$ to $-8‰$; $\delta^{15}N = -2$ to $-9‰$ [1]; $^{40}Ar/^{36}Ar \leq 40\,000$; $^{3}He/^{4}He$ 4–8 Ra; $^{20}Ne/^{22}Ne \leq 11$; ^{129}Xe excess [3–6]). Coated diamonds from Africa contain CO_2–H_2O bearing micro-inclusions rich in water, carbonate, silica and show similar chemical trends for samples from different locations [2,7,8]. Recently upper mantle fluids have also been detected in cloudy diamond monocrystals from Koffiefontein that have extended the range in composition with notably high contents of water, Cl and K [9].

The inclusions in fibrous coats contain polyphase assemblages of daughter minerals including quartz, phyllosilicates, carbonates and apatite [2,7,10–13]. The genesis age of the coats is not well-constrained; based on Sr isotopes analyses, Akagi and Masuda [14] have suggested a maximum age of 500 Ma for Zairian coated diamonds. Previous Ar–Ar analyses of Zaire coats could only constrain the age to < 4 Ga [3,15]. The aggregation state of nitrogen impurities in the coats of African diamonds is Type IaA [1] suggestive of a relatively short mantle residence time. This has been used as a strong argument for the coat-forming event being closely related in time to kimberlite magmatism [1,16].

We have investigated the noble gas and halogen geochemistry of fluids trapped in coated diamond using extension of the Ar–Ar technique [3,17,18]. Neutron irradiation produces noble gas isotopes from Cl, Br and I (and K, Ca, Ba, U). Previously we have shown that coated diamonds from Africa (Democratic Republic of Congo and Botswana) have a relatively restricted range in halogen ratios ($Br/Cl = 1$–2×10^{-3} M; $I/Cl = 20$–70×10^{-6} M) that are similar to MORB values [3,17,18]. This is in strong contrast to the highly variable halogen ratios measured in Canadian coated diamonds ($Br/Cl = 1$–63×10^{-3} M; $I/Cl = 10$–2000×10^{-6} M) which are considered to reflect halogen fractionation occurring during localised crystallisation of a Cl bearing phase (e.g. apatite) in the diamond source region [18]. Previous studies also reveal a narrow range of $^{40}Ar*/Cl$ in coated diamonds between 500 and 1400×10^{-6} M, consistent with noble gases and halogens being present in a mantle fluid phase [3,15,18]. Studies of coated diamonds are therefore providing an emerging picture of mantle halogen geochemistry that can be used to understand the exchange of these volatiles between the mantle and exosphere, including their accumulation in surface reservoirs via outgassing of the Earth's interior, their degree of mantle depletion and recycling back into the mantle.

The problem of determining the composition of halogens in the mantle is not straightforward as a large proportion of these elements are presently trapped at the Earth's surface mainly in the oceans (Cl and Br) and sediments (I). The concentrations in mantle materials are therefore low (a few ppm to ppb) and difficult to measure accurately using conventional techniques. Direct determination of halogens from mantle materials is rare and, apart from diamonds, most of our understanding comes from analyses of MORB [19–21]. Halogens in MORB suffer from problems related to contamination with seawater and fractionation during shallow magma degassing [21,22]. These processes lead to halogen concentrations varying by factors of 10–100 in these rocks [19–21]. Since diamonds form in the subcontinental lithospheric mantle and are only stable at depths below 150 km, they are not directly affected by seawater contamination or degassing.

In this paper we report halogen (Cl, Br, I) and Ar isotope data for coated diamonds from the Aikhal kimberlite, Siberia, Russia and a few additional samples from African and Canadian sources. From these analyses we assess the age of the coat-forming event, and estimate the abundance of halogens in the diamond-forming regions of the mantle.

2. Experimental methods

Seven coated diamonds from Siberia, Russia (Aikhal kimberlite, Alekit field, Siberian craton) and two each from the Democratic Republic of Congo (DRC) and Canada (Leslie and Koala kimberlites, North West Territories) were analysed by extension of the Ar–Ar method for noble gases (Ar, Kr and Xe) and halogens (Cl, Br and I). The Aikhal diamonds were either green or grey

in colour and weighed between 0.032 and 0.047 g. The DRC and Canadian diamonds are additional samples from a previously described sample set [18].

Diamonds were irradiated in position L67 of the Ford Reactor, Michigan, USA with a fast neutron flux of 3.2×10^{18} cm^{-2} and thermal flux of 8.7×10^{18} cm^{-2} as determined from Hb3gr monitors that were included in the irradiation package. Following irradiation the samples were analysed in one of two ways: (1) five of the Aikhal diamonds (A3, A4, A5, A6 and A7) were step-heated over the interval 400–2150°C; (2) the African, Canadian and two remaining Siberian diamonds (A1 and A2) were broken into between two and seven fragments and each was analysed in a single temperature step at 2100°C.

Stepped heating of whole stones has the advantage of minimising the effects of any adsorbed atmospheric noble gases that are usually released at relatively low temperature, and has the potential ability to distinguish between different noble gas components (e.g. from minerals or inclusions) present in the diamond. However, diamonds usually release noble gases in only one or two temperature steps (1600°C and 2000°C [18]) so only an average composition is obtained. Use of a laser probe is superficially appealing for its high spatial resolution, but is restricted by the detection limits for the heavy halogens especially iodine [18].

The analysis of multiple fragments of each diamond enables more measurements from each sample and makes it possible to test for the internal compositional homogeneity of each diamond. Another advantage of analysing fragments is that it avoids potential problems of ^{39}Ar recoil during irradiation from K-rich fluid inclusions into the diamond matrix, which may then be released over different temperature intervals. The analysis of small diamond samples weighing 0.1–2 mg is possible because the detection limits for Cl (10^{-10} g), Br (10^{-12} g) and I (10^{-12} g) are 10–100 times lower using the Ar–Ar technique than with conventional techniques. Experimental procedures, blanks and data reduction methods used have been described previously [18]. Argon blanks are low, typically $< 1\%$ of the total gas released from the diamonds, and are isotopically indistinguish-

able from air. Blank corrections simply move data along an air-mantle mixing line and add to the uncertainty of the isotopic ratios and therefore have not been applied to the data. Ratios involving elements (Cl, Br, I, Ca, K) and isotopes (^{40}Ar, ^{36}Ar) are molar and errors are one standard deviation.

3. Results

3.1. Siberian coated diamonds

Stepped heating of five Aikhal diamonds gives a bimodal release of noble gases at 1600°C (15–30%) and above 2000°C (70–85%), similar to that observed previously for African and Canadian diamonds [18]. The major release at > 2000°C corresponds to graphitisation. The cause of the release at 1600°C is not well-understood; it may be related to rupture of inclusions in the diamond or be associated with neutron-induced radiation damage during irradiation. However, the isotopic and chemical compositions of gases released at low and high temperature are indistinguishable and data are summarised in Table 1. Total concentrations of noble gases and halogens in Siberian diamonds are about 5 times lower than in African diamonds and 50 times below those measured in Canadian diamonds (see Tables 1 and 2). The most likely reason for this difference is a lower population density of inclusions in the Siberian diamonds.

Siberian coated diamonds show a good correlation on a ^{40}Ar/^{36}Ar–Cl/^{36}Ar plot (Fig. 1) indicating mixing between a component having low ^{40}Ar/^{36}Ar ~ 300 and Cl/^{36}Ar = 0, with a component having high ^{40}Ar/^{36}Ar ≥ 5000 and high Cl/^{36}Ar $\geq 10 \times 10^6$. Because the data have not been corrected for blanks, the most likely origin of the low ^{40}Ar/^{36}Ar component is blank from the furnace system or adsorbed air on the samples. This is consistent with this component being released predominantly at low temperature from those samples that were subjected to stepped heating. The excess ^{40}Ar and Cl-rich component has a uniform ^{40}Ar*/Cl ratio, both within and between individual diamonds, given by the slope of the

Table 1
Russian diamond Ar–Ar stepped heating data

Sample	Wt mg	Cl ppm	Br ppb	I ppb	K ppm	Ca ppm	U ppb	Br/Cl $\times 10^{-3}$ M	I/Cl $\times 10^{-6}$ M	K/Cl M	^{36}Ar $\times 10^{-15}$ mol/g	^{40}Ar $\times 10^{-12}$ mol/g	^{84}Kr $\times 10^{-15}$ mol/g	^{132}Xe $\times 10^{-15}$ mol/g	^{40}Ar*/Cl $\times 10^{-6}$ mol/g
Bulk															
A1	36.1	4.0±0.1	15.4±0.3	0.33±0.05	37.5±0.3	na	72±4	1.71±0.04	23.0±3.5	8.5±0.1	130±2	98.0±0.1	1.00±0.01	0.21±0.02	528±6
A2	46.8	6.8±0.1	24.6±0.2	0.54±0.04	41.0±0.3	na	46±2	1.59±0.02	21.8±1.5	5.4±0.1	68±2	118.0±0.1	1.40±0.05	0.16±0.03	506±3
A3	42.3	5.9±0.1	20.4±0.2	0.43±0.01	62.1±0.7	49±3	7±2	1.53±0.03	20.3±0.5	9.5±0.2	25±3	111.4±0.5	1.35±0.02	0.15±0.01	620±9
A4	31.5	11.2±0.1	52.4±0.3	0.91±0.05	68.0±0.8	94±5	18±1	2.07±0.02	22.6±1.4	5.5±0.1	33±3	163.7±0.5	2.26±0.02	0.28±0.01	488±5
A5	42.6	5.2±0.1	21.5±0.1	0.39±0.01	29.9±0.4	26±3	8±1	1.83±0.03	20.7±0.5	5.2±0.1	19±2	83.0±0.1	1.47±0.05	0.15±0.01	525±7
A6	57.9	4.5±0.1	17.2±0.2	0.46±0.01	54.3±0.5	61±2	14±1	1.68±0.02	28.3±0.7	10.8±0.2	24±2	81.8±0.3	0.86±0.03	0.19±0.01	581±7
A7	47.1	14.7±0.1	59.2±0.7	0.90±0.03	100.7±0.9	62±3	12±2	1.79±0.03	17.0±0.6	6.2±0.1	51±2	241.0±0.8	1.25±0.05	0.22±0.01	545±5
Average		7.5±4.0	30±17	0.57±0.24	56.2±23.9	58±25	25±24	1.74±0.18	22.0±3.4	7.3±2.3					542±45
Fragments															
A1/a	6.9	3.0±0.1	8.2±0.5	nd	33.5±0.6	na	20±2	1.21±0.08	nd	9.8±0.4	92±5	79.3±0.1	5.37±0.08	0.27±0.01	605±22
A1/b	7.4	3.0±0.1	9.5±0.6	nd	35.1±0.5	na	14±5	1.39±0.09	nd	10.3±0.4	87±7	76.4±0.1	3.91±0.04	0.43±0.01	595±19
A1/c	6.1	2.8±0.1	9.4±0.8	0.64±0.22	26.0±0.9	na	195±15	1.51±0.14	64.1±22.0	8.3±0.4	180±7	97.6±0.1	11.67±0.12	5.88±0.01	567±19
A1/d	10.4	5.1±0.1	27.0±0.7	0.47±0.06	42.3±0.5	na	48±5	2.32±0.08	25.2±3.4	7.3±0.2	140±4	107.4±0.1	6.19±0.01	1.73±0.01	455±9
A1/e	5.8	5.7±0.1	17.0±0.7	0.47±0.13	55.3±0.8	na	125±10	1.32±0.06	22.9±6.5	8.6±0.2	164±6	134.5±0.1	9.26±0.09	3.57±0.01	535±10
A2/a	9.7	7.5±0.1	26.1±0.5	0.57±0.06	45.1±0.7	na	22±2	1.54±0.04	21.0±2.4	5.4±0.1	48±3	125.8±0.1	2.79±0.05	0.49±0.01	526±9
A2/b	8.8	7.1±0.1	30.3±0.2	0.46±0.14	39.7±0.5	na	21±4	1.89±0.03	18.0±5.4	5.1±0.1	71±4	119.1±0.1	3.21±0.04	0.65±0.01	488±8
A2/c	6.8	7.3±0.1	27.2±0.4	0.69±0.10	43.0±0.7	na	77±6	1.64±0.03	26.3±3.9	5.3±0.1	66±6	125.6±0.1	5.12±0.05	3.01±0.01	512±7
A2/d	10.4	5.1±0.1	16.7±0.2	0.55±0.06	31.1±0.4	na	58±8	1.47±0.03	30.4±3.2	5.6±0.1	59±3	88.7±0.1	3.55±0.04	2.17±0.01	500±7
A2/e	4.1	9.0±0.1	25.6±1.1	0.21±0.11	51.9±0.9	na	25±10	1.26±0.06	6.4±3.3	5.2±0.1	112±7	157.0±0.1	5.01±0.08	0.78±0.01	487±7
A2/f	7.1	6.5±0.1	23.6±0.3	0.60±0.03	43.2±0.8	na	74±4	1.60±0.04	25.8±1.3	6.0±0.2	81±6	119.2±0.1	4.84±0.05	2.20±0.01	516±9

Errors are 1σ.
nd, not determinable (1σ error > 30%).
na, not analysed.

correlation in Fig. 1 of $527 \pm 22 \times 10^{-6}$. The high $^{40}Ar/^{36}Ar$ ratio of this component, reaching 11 000 at high temperature during stepped heating, is comparable to estimates for the $^{40}Ar/^{36}Ar$ in the upper mantle. Fig. 2 is a summary $^{40}Ar/^{36}Ar–Cl/^{36}Ar$ plot for diamonds from wide geographical distribution and shows that the $^{40}Ar*/Cl$ value for Siberian diamonds is at the lower end of the range measured previously in African and Canadian diamonds ($506–1347 \times 10^{-6}$ [18]).

Analyses of fragments of diamonds A1 and A2 do not reveal significant variations in $^{40}Ar*/Cl$ values (Fig. 1) or halogen ratios, although the concentrations of noble gases and halogens in different fragments vary by up to a factor of 3 (Table 1). Each fragment being a mixture of differing proportions of inclusion-rich coat and inclusion-poor core diamond explains this variation.

Bulk halogen ratios are uniform within and between the seven Aikhal diamonds with average $Br/Cl = 1.74 \pm 0.18 \times 10^{-3}$ and $I/Cl = 22.0 \pm 3.4 \times 10^{-6}$ (Fig. 3 and Table 1). These values are indistinguishable from those of African diamonds (Botswana and Zaire) which have $Br/Cl = 1.56 \pm 0.25 \times 10^{-3}$ and $I/Cl = 20–70 \times 10^{-6}$ [18]. The diamond I/Cl is within the range estimated for MORB of $15–25 \times 10^{-6}$ (see [18] for discussion), however Br/Cl of MORB is lower at $1.03 \pm 0.29 \times 10^{-3}$ [21].

3.2. African and Canadian diamonds

The results are in agreement with our previous studies of diamonds from these sources [18]. The most important finding is the large variation in $^{40}Ar*/Cl$ obtained for DRC diamond CT1 with seven fragments of this sample showing a range of values between 886 and 2024×10^{-6} (Fig. 1). This exceeds the range measured in other DRC diamonds by stepped heating of $547–1358 \times 10^{-6}$ [18], although the bulk value for CT1 of 1145×10^{-6} is within this range. The variation in $^{40}Ar*/Cl$ is not correlated with changes in K/Cl or K concentration suggesting that differences are not related to $^{40}Ar*$ produced by in situ radioactive decay in K-rich inclusions. Previously this diamond was analysed using a laser probe but did not reveal any variations in $^{40}Ar*/Cl$ outside of

experimental error with an average of $876 \pm 17 \times 10^{-6}$ [18]. The results of the laser probe analyses suggest that the different $^{40}Ar*/Cl$ values of fragments are not related to systematic radial variations of this ratio in the coat itself, but rather that coat and core regions of the diamond have distinct $^{40}Ar*/Cl$ values. A few laser probe analyses of the core of CT1 were made but did not release significant amount of Ar, however it is likely that Ar is concentrated in fractures running through the core. Each fragment is likely to be a mixture of coat and core material thus explaining the variable $^{40}Ar*/Cl$ values obtained by furnace heating. Fragments of the other DRC diamond (CT3) and a Canadian sample (SK8C/21) show relatively uniform $^{40}Ar*/Cl$ values. It is interesting to speculate on how much of the apparent $^{40}Ar*/Cl$ variation between African coated diamonds, and perhaps those from Canada (Fig. 2), results from internal variations within individual stones like that observed for CT1. The analysis of fragments from a single diamond therefore appears to a be useful method for revealing internal complexity in ^{40}Ar abundance that is not apparent from stepped heating of whole samples.

Halogen ratios of African and Canadian diamonds (Table 2) are consistent with the previously reported range of determinations [18]. The notable feature is the extremely high Br/Cl and I/Cl ratios of the Canadian stones compared to Siberian and African diamonds and MORB values (Fig. 3).

4. Discussion

4.1. Age constraints of Siberian coated diamonds

We are not aware that any age determinations have been reported for the Aikhal kimberlite. Radiometric ages (U–Pb, Rb–Sr and K–Ar) of eight other kimberlite pipes in the Alekit kimberlite field have been compiled by Griffin et al. ([23], and references therein) and show a narrow span of 350–380 Ma. SHRIMP U–Pb analyses of two zircons from the Aikhal kimberlite give much older ages at 1890 Ma but are considered to be xenocrysts from surrounding granites [23].

Table 2
African and Canadian diamond Ar–Ar stepped heating data

Sample	Wt mg	Cl ppm	Br ppb	I ppb	K ppm	U ppb	Br/Cl $\times10^{-3}$ M	I/Cl $\times10^{-6}$ M	K/Cl M	^{36}Ar $\times10^{-15}$ mol/g	^{40}Ar $\times10^{-12}$ mol/g	^{84}Kr $\times10^{-15}$ mol/g	^{132}Xe $\times10^{-15}$ mol/g	^{40}Ar*/Cl $\times10^{-6}$ M
Africa														
CT1/a	3.0	29.9 ± 0.8	77.1 ± 0.9	2.3 ± 0.3	182.7 ± 5.0	261 ± 32	1.14 ± 0.03	21.6 ± 2.9	5.5 ± 0.2	669 ± 10	957.1 ± 2.1	24.8 ± 0.4	6.95 ± 0.01	897 ± 24
CT1/b	4.7	21.7 ± 0.6	66.5 ± 1.9	2.3 ± 0.1	126.4 ± 3.2	77 ± 10	1.35 ± 0.05	29.6 ± 1.6	5.3 ± 0.2	356 ± 11	939.4 ± 1.6	11.4 ± 0.1	2.65 ± 0.01	1358 ± 37
CT1/c	3.5	8.7 ± 0.3	20.5 ± 0.7	1.7 ± 0.1	47.3 ± 1.6	554 ± 11	1.04 ± 0.05	53.8 ± 3.6	4.9 ± 0.2	717 ± 17	434.4 ± 0.6	36.4 ± 0.3	15.74 ± 0.01	903 ± 32
CT1/d	3.8	30.7 ± 0.8	81.9 ± 1.9	2.4 ± 0.3	188.2 ± 5.5	120 ± 7	1.18 ± 0.04	21.7 ± 2.4	5.5 ± 0.2	468 ± 8	1016.0 ± 2.0	14.1 ± 0.1	2.70 ± 0.01	1010 ± 27
CT1/e	4.9	14.0 ± 0.4	32.5 ± 1.2	1.6 ± 0.1	76.2 ± 2.1	3 ± 8	1.02 ± 0.05	31.6 ± 1.3	4.9 ± 0.2	390 ± 14	480.0 ± 0.8	11.9 ± 0.1	2.72 ± 0.01	919 ± 27
CT1/f	4.6	24.4 ± 0.6	64.4 ± 1.1	2.5 ± 0.1	138.7 ± 3.7	4 ± 18	1.17 ± 0.04	28.4 ± 1.7	5.1 ± 0.2	408 ± 11	732.7 ± 1.3	15.7 ± 0.1	5.60 ± 0.01	886 ± 23
CT1/g	4.5	17.3 ± 0.5	54.1 ± 1.6	1.8 ± 0.1	99.0 ± 2.7	nd	1.38 ± 0.06	28.7 ± 1.1	5.2 ± 0.2	295 ± 10	1077.8 ± 1.9	10.3 ± 0.1	2.53 ± 0.01	2024 ± 54
Total		20.6 ± 0.2	56.0 ± 0.6	2.1 ± 0.1	119.7 ± 1.3	121 ± 5	1.20 ± 0.02	28.0 ± 0.8	5.3 ± 0.1	451 ± 5	800.2 ± 0.6	16.7 ± 0.1	5.43 ± 0.01	1145 ± 16
CT3/a	5.9	16.4 ± 0.4	53.4 ± 1.3	2.6 ± 0.1	83.9 ± 2.5	90 ± 4	1.44 ± 0.05	43.5 ± 2.1	4.6 ± 0.2	149 ± 7	458.6 ± 1.0	6.2 ± 0.1	1.22 ± 0.01	891 ± 24
CT3/b	8.7	7.7 ± 0.2	26.9 ± 0.5	1.5 ± 0.1	38.1 ± 1.0	48 ± 2	1.54 ± 0.05	55.0 ± 4.4	4.5 ± 0.1	83 ± 4	228.6 ± 0.4	3.9 ± 0.1	1.24 ± 0.01	933 ± 25
CT3/c	7.8	26.0 ± 0.9	79.6 ± 1.4	2.5 ± 0.1	136.7 ± 5.0	82 ± 8	1.35 ± 0.05	27.0 ± 1.8	4.7 ± 0.2	91 ± 7	646.7 ± 14.1	3.2 ± 0.1	0.82 ± 0.01	842 ± 39
CT3/d	4.3	25.9 ± 0.9	93.8 ± 1.3	2.8 ± 0.2	127.9 ± 4.3	62 ± 9	1.60 ± 0.05	29.6 ± 2.7	4.5 ± 0.2	154 ± 8	709.0 ± 15.4	5.9 ± 0.1	0.94 ± 0.01	905 ± 36
CT3/e	5.1	35.2 ± 1.2	126.5 ± 1.1	3.4 ± 0.3	191.6 ± 6.4	52 ± 13	1.59 ± 0.06	26.8 ± 2.7	4.9 ± 0.2	148 ± 8	888.0 ± 19.2	5.4 ± 0.1	1.23 ± 0.01	849 ± 39
Total		20.7 ± 0.3	69.7 ± 0.5	2.4 ± 0.1	107.5 ± 1.8	67 ± 3	1.49 ± 0.03	32.7 ± 1.2	4.7 ± 0.1	117 ± 3	544.2 ± 5.1	4.7 ± 0.1	1.01 ± 0.01	871 ± 16
Canada[a]														
SK8C/21/a	0.8	217.7 ± 6.6	2.2 ± 0.1	1055 ± 48							2469.8 ± 20.1	33.5 ± 1.6	520.9 ± 14.8	240 ± 80
5.02 ± 0.16		42.9 ± 2.4									9166.3 ± 13.3	31.5 ± 0.8	5.46 ± 0.03	1438 ± 47
SK8C/21/ b	0.7	199.0 ± 6.0									2393.9 ± 20.5	31.9 ± 2.5	466.7 ± 13.2	349 ± 34
5.32 ± 0.17		44.6 ± 3.7	2.1 ± 0.1	943 ± 61							7970.1 ± 14.2	31.8 ± 0.7	5.45 ± 0.03	1366 ± 41
SK8C/21/c	1.1	234.9 ± 7.4									3030.2 ± 15.5	35.5 ± 1.9	507.0 ± 25.8	35 ± 9
5.71 ± 0.18		42.1 ± 2.6	2.0 ± 0.1	863 ± 46							10434.5 ± 14.9	30.4 ± 0.6	5.00 ± 0.03	1532 ± 49
Total		220.4 ± 4.1									2692.2 ± 10.6	34.0 ± 1.1	501.1 ± 12.5	180 ± 27
5.41 ± 0.10		42.9 ± 1.7	2.1 ± 0.1	943 ± 30	9408.5 ± 8.5									
SLEB32	1.5	9.2 ± 0.6	227.4 ± 1.3	10.3 ± 0.4	41.1 ± 3.2	65 ± 11	31.1 ± 0.4				311.7 ± 25.4	4.0 ± 0.4	157 ± 18	484.2 ± 0.7
6.0 ± 0.1		1.82 ± 0.01	1679 ± 12				10.91 ± 0.76	5.26 ± 0.03	1465 ± 27					

Errors are 1σ.

[a] SK8C/21 Koala; SLEB32 Leslie.
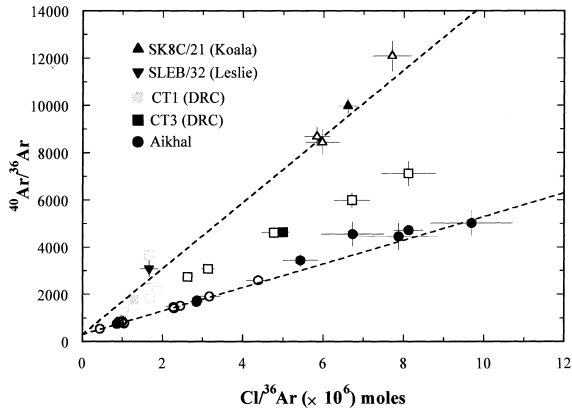
Fig. 1. $^{40}Ar/^{36}Ar$ versus $Cl/^{36}Ar$ for Siberian (Aikhal), DRC and Canadian (Koala and Leslie) coated diamonds obtained by stepped heating of whole diamonds (solid symbols) and fragments (open symbols). The linear correlation shown by Siberian diamonds indicates mixing between a low $^{40}Ar/^{36}Ar$ component (293 ± 29), probably adsorbed atmospheric Ar on the samples or furnace blank, and a mantle-derived ^{40}Ar excess component with high $^{40}Ar/^{36}Ar \geq 5000$ and high $Cl/^{36}Ar \geq 10 \times 10^6$. This component has a uniform $^{40}Ar*/Cl$ value given by the slope of the linear correlation of $527 \pm 22 \times 10^{-6}$. Coated diamonds from other sources show higher $^{40}Ar*/Cl$ values, but note the variable $^{40}Ar*/Cl$ values obtained for fragments from CT1. Dashed lines are shown for $^{40}Ar*/Cl$ at 500×10^{-6} and 1500×10^{-6}.

Apparent K–Ar isochrons (e.g. on plots of $^{40}Ar/^{36}Ar$ versus $K/^{36}Ar$ but not shown here) give ages of 3–4 Ga for the Aikhal coated diamonds. However, these old apparent ages do not represent the time of diamond growth and can be explained by the presence of a substantial concentration of K in a mantle fluid containing at least two Ar components. The major Ar bearing component is excess ^{40}Ar characterised by a uniform $^{40}Ar*/Cl$ in the fluid phase as described earlier. Clues to the identity of at least one other Ar component is revealed using multi-element correlations involving $^{40}Ar*$, Cl and K. A small correction for the presumed atmospheric ^{40}Ar has been applied to the data shown in Fig. 4 in which $^{40}Ar*/K$ is plotted against Cl/K. We emphasise that because we have only plotted data for whole stones and diamond fragments in Fig. 4, the variation in Cl/K and $^{40}Ar*/K$ can not be attributed to an experimental artefact caused by recoil of $^{39}Ar_K$ from the fluid into the K-poor diamond matrix.

In Fig. 4, the variation in Cl/K between diamonds (and also Ca/K which ranges between 0.6

Fig. 2. $^{40}Ar/^{36}Ar$ versus $Cl/^{36}Ar$ for coated diamonds from Africa (Jwaneng and DRC), Canada (Fox, Grizzly, Koala and Leslie) and Russia (Aikhal). Open symbols are maximum values obtained during stepped heating analysis usually from gas released at 2000–2100°C. For African and Canadian sources the open symbols are from previously published data [3,18]. Solid symbols are total values obtained by summing the gas released over all the temperature intervals and are from diamonds analysed in the present study. It is notable that all data have $^{40}Ar*/Cl$ values between 500 and 1500×10^{-6} shown by dashed lines.
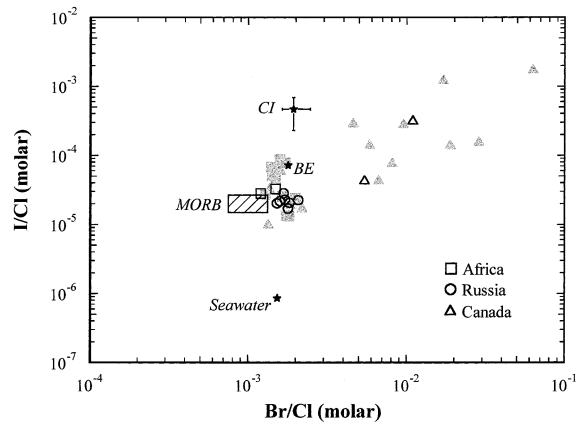

Fig. 3. Molar ratios of I/Cl versus Br/Cl for Siberian, Canadian and African diamonds. Open symbols are results from this study, solid grey symbols are published data for African and Canadian coated diamonds from Johnson et al. [18]. Halogen ratios of Siberian diamonds are uniform and similar to those obtained from African sources. The MORB field is obtained from published data [20,21]. CI is the carbonaceous chondrite value where bars indicate the range of data for Orgueil and Ivuna [36]. BE is the bulk Earth halogen composition estimated using data from coated diamonds (see text for discussion).

and 1.3) is caused either by the mixing of mantle fluids of differing chemical composition, or by localised chemical fractionation between fluids and solids during crystallisation of diamond coats. In contrast, the variation in $^{40}Ar^*/K$ may result from radiogenic ^{40}Ar formed by in situ decay of ^{40}K present in the fluid inclusions in the coats. In this scenario, the correlation shown in Fig. 4 is interpreted as a mixing line between an excess ^{40}Ar-rich component having a high Cl/K ≥ 0.19 and constant $^{40}Ar^*/Cl$ value, with a radiogenic ^{40}Ar component with Cl/K ≤ 0.09 and $^{40}Ar^*/K \leq 53.85 \times 10^{-6}$. This $^{40}Ar^*/K$ corresponds to an age of 3.04 Ga and represents the *maximum* time of coat growth. The *minimum* $^{40}Ar^*/K$ of the radiogenic component is obtained from Fig. 4 by extrapolation of the mixing line to the intercept (Cl/K = 0). The regression line gives $^{40}Ar^*/K = 15.29 \pm 1.20 \times 10^{-6}$ formally equivalent to an age of 1.44 ± 0.17 Ga. However the $^{40}Ar^*/Cl$ given by the slope is only 435×10^{-6}, considerably below that measured in any of the diamonds (Table 1). For this reason it is considered that the linear fit is unreliable and the apparent age of 1.44 Ga has no geological significance. Linear regression using a fixed intercept of $^{40}Ar^*/K = 2.87 \times 10^{-6}$, equivalent to the most likely age

Fig. 4. $^{40}Ar^*/K$ versus Cl/K for Aikhal coated diamonds. Solid symbols are total release data, open symbols were obtained from diamond fragments. The correlation is interpreted to indicate mixing between fluids with a relatively constant $^{40}Ar^*/Cl$ ratio and variable Cl/K. The linear regression line is for an intercept of $^{40}Ar^*/K = 2.87 \times 10^{-6}$ equivalent to an age of 380 Ma considered to be the most likely time of kimberlite emplacement.

for the host kimberlite of 380 Ma, gives a slope $^{40}Ar^*/Cl = 508 \times 10^{-6}$. This $^{40}Ar^*/Cl$ is within error of the value obtained from the $^{40}Ar/^{36}Ar$–Cl/^{36}Ar correlation of $527 \pm 22 \times 10^{-6}$ (shown in Fig. 1). Alternatively, setting the slope $^{40}Ar^*/Cl = 527 \times 10^{-6}$ gives an intercept $^{40}Ar^*/K = 9.25 \times 10^{-7}$ equivalent to an age of just 131 Ma. This age is outside the range of eruption ages for kimberlites of the Alekit field (350–380 Ma), and therefore is considered unlikely to represent the time of kimberlite emplacement.

In summary, the minimum age of coat growth implied by the $^{40}Ar^*/K$ of the radiogenic component is most consistent with an age of 350–380 Ma which is probably when the host kimberlite was emplaced. This would imply that there is a genetic link between kimberlite magmatism and the growth of diamond coats. From here on the chronological interpretation is discussed in terms of published age information for other sources of Siberian diamonds and its relevance to the nitrogen aggregation state of fibrous diamonds.

A Re–Os model age of 3.4 Ga has been reported for a peridotitic sulphide inclusion from an Aikhal diamond monocrystal [24]. Analysis of inclusion bearing diamonds from Udachnaya, another Siberian kimberlite, yielded ages of 3.1–3.5 Ga (Re–Os model ages, peridotitic suite sulphide inclusions; [25]) and 2.01 ± 0.060 Ga (Sm–Nd isochron, harzburgitic suite; [26]). A strong link between coated diamonds and eclogitic paragenesis of diamonds has been suggested [7]. Burgess et al. [27] attempted to determine the age of a buried clinopyroxene inclusion in an eclogitic diamond from Udachnaya using the laser Ar–Ar technique and obtained an age of 1149 ± 74 Ma; while eclogitic sulphide inclusions from Mir diamonds gave an Re–Os age of 323 ± 22 Ma close to the host kimberlite eruption age [24].

Further insight into the age of diamond coats can be obtained from their nitrogen aggregation state. Although the nitrogen aggregation state in diamond coats from Aikhal has not been determined, in other Siberian coats it is Type IaA [28] the same as found in diamond coats elsewhere in the world. This compares with the higher aggregation states of Type IaA platelets to pure Type IaB platelets in the cores of coated diamonds.
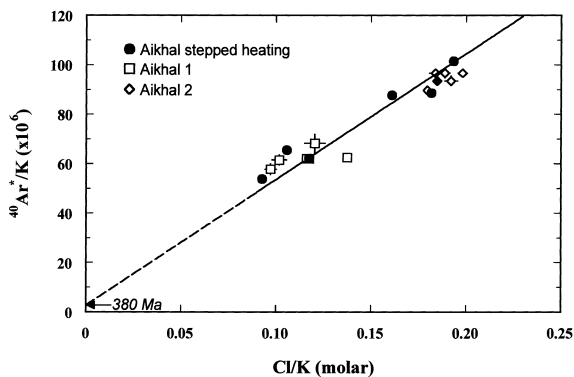
Since for a given concentration of nitrogen, the rate of aggregation depends upon time and temperature, the cores are assumed to be older than the coats. Furthermore, the global uniformity of Type IaA aggregation in diamond coats has been used as evidence for a causal relationship between kimberlite magmatism and coat growth [1,15]. A relatively short time period between growth of the coats and eruption of the kimberlite, necessary to enable a small degree of nitrogen aggregation, is consistent with the chronological interpretation of the Ar/K/Cl data given earlier.

4.2. Halogen composition of the mantle determined from diamonds

The close similarity in $^{40}Ar^*/Cl$, Br/Cl and I/Cl for African and Siberian diamonds implies a wide-scale homogeneity of halogen composition in the sub-continental mantle. The diamond halogen ratios also closely match those determined for the present day MORB source. The correlation between noble gas isotopes and halogens exemplified by the uniform $^{40}Ar^*/Cl$ ratio in Siberian diamonds, and the limited variation in this ratio in diamonds from sources that are geographically widespread, provides a means to determine the depleted mantle halogen composition if the $^{40}Ar^*$ of the upper mantle can be independently determined. The median $^{40}Ar^*/Cl$ ratio of African diamonds is 950×10^{-6} M with about 40% variation around this value (Fig. 2). Estimation of the $^{40}Ar^*$ content of the upper mantle is obtained from the degassing flux of He and Ar at mid-ocean ridges. The ^3He flux at ridges has been determined at 1000 mol/yr with a $^4He/^3He$ ratio of 90 000 [29,30] and $^{40}Ar^*/^4He$ of about 0.5 [31]. The $^{40}Ar^*$ degassing flux is therefore estimated to be 4.5×10^7 mol/yr. MORB is produced at a rate of 20 km^3/yr, has a density of 3.2 g/cm^3 and represents 5–15% partial melt, so the $^{40}Ar^*$ content of the MORB source is calculated to be 7.03×10^{-11} mol/g. Combining this estimate with $^{40}Ar^*/Cl$ of 950×10^{-6} obtained from coated diamonds gives a Cl content of 3 ppm. This Cl abundance is in very good agreement with previous determinations for the oceanic depleted upper mantle. Based on abundances in MORB glasses

and model calculations, Schilling et al. [19] obtained a value of 7 ppm Cl for the upper mantle, and Jambon et al. [21] reported a value of 55 ppm Cl for N-MORB samples equivalent to a MORB mantle source value of approximately 6 ppm Cl.

Estimates of the Br and I contents of the diamond source region can be made using the Cl abundance and the average Br/Cl = 1.65×10^{-3} (n = 21) and I/Cl = $36 \pm 21 \times 10^{-6}$ (n = 19) for African and Siberian diamonds. This yields 11 ppb Br and 0.4 ppb I for the sub-continental mantle. These values compare favourably with previous estimates of the MORB mantle source region of 8 ppb Br [21] and ≥ 0.8 ppb I [20].

4.3. Bulk silicate Earth halogen budget

The halogen abundances of the upper mantle derived from diamonds can be used to estimate their concentration in the bulk silicate Earth by summing the amount of halogens stored in surface reservoirs (crust, sediments and seawater) and the depleted upper mantle. It is further assumed that the depleted mantle represents one third of the entire mantle. For surface reservoirs we use Cl and Br abundances given by Schilling et al. [32] and I data of Muramatsu and Wedepohl [33]. When these data are combined with upper mantle estimates based on diamond coats, bulk Earth halogen abundances of 27 ppm Cl, 108 ppb Br and 7 ppb I are obtained. These values are consistent with estimates based on MORB of Cl = 35 ± 5 ppm, Br = 100 ± 15 ppb [21] and I = 10 ppb [20]. However, the most recent published estimates, based on meteorite data and condensation temperatures, predict higher bulk Earth values Br = 400 ppb and I = 40 ppb, but a similar value for Cl of 10 ppm [34]. The halogen abundances indicate that > 90% of the halogens from the upper mantle have been transferred to the crust and ocean with the proportion degassed increasing in the order Cl < Br < I. Organic-rich sediments contain about 90% of the surface I so it is possible that during the early period of Earth history I may have accumulated in the ocean similar to Cl and Br at the present day. Iodine would not have been transferred and stabilised in sediments until the formation of an early continental

crust, which may have occurred as soon as 4.4 Ga [35], or not until after the emergence of ocean life.

The bulk Earth halogen abundances calculated from diamonds are about 25–30× lower for Cl and Br and 160× lower for I compared to CI carbonaceous chondrites (Fig. 3); a reflection of the highly volatile nature of these elements. While the Br/Cl ratio of the bulk Earth (1.77×10^{-3}) is comparable to CI chondrites ($1.64 \pm 0.9 \times 10^{-3}$ [36]), the I/Cl appears to be about a factor of 6 lower (Fig. 3; 72×10^{-6} bulk Earth versus $467 \pm 22 \times 10^{-6}$ CI chondrite [36]). This may not transpire to be a serious discrepancy for I abundance in the Earth because I/Cl values have been measured in only two CI chondrites and they are dissimilar at 693×10^{-6} in Ivuna and 231×10^{-6} in Orgueil [36].

5. Conclusions

Results of Ar–Ar stepped heating experiments of Aikhal diamonds indicate the presence of at least three distinct Ar components:

1. The major Ar bearing phase is characterised by high Cl/K and high $^{40}Ar/^{36}Ar$ and a uniform $^{40}Ar*/Cl$ value ($527 \pm 22 \times 10^{-6}$). The ^{40}Ar is interpreted as excess ^{40}Ar present in a widespread Cl-rich fluid phase. The fluid has uniform Br/Cl ($1.74 \pm 0.18 \times 10^{-3}$) and I/Cl ($22.0 \pm 3.4 \times 10^{-6}$) similar to the fluid phase in African and some Canadian coated diamonds and halogens in MORB. Data from coated diamonds can be used to constrain the halogen abundances in the sub-continental mantle at 3 ppm Cl, 11 ppb Br and 0.4 ppb I. These estimates imply that the upper mantle is >90% degassed of its halogens.
2. A second Ar component is characterised by low Cl/K and a $^{40}Ar*/K$ that is most easily explained by in situ decay of ^{40}K in the fluid inclusions. Mixing of mantle fluids with different composition or chemical fractionation during the localised crystallisation of solid phases leaving the fluid variably depleted in Ca and K is the most probable reason for the K/Cl and Ca/Cl variations between diamonds. The mini-

mum age of coat growth implied by the $^{40}Ar*/$ K implies the diamond coats grew just prior to kimberlite eruption most probably between 350 and 380 Ma ago.
3. A third component is characterised by a low $^{40}Ar/^{36}Ar$ ratio of around 300 and is predominantly released at low temperature. The simplest interpretation of this component is adsorbed atmospheric Ar on the diamond samples.

References

[1] S.R. Boyd, F. Pineau, M. Javoy, Modelling the growth of natural diamonds, Chem. Geol. 116 (1994) 29–42.
[2] O. Navon, I.D. Hutcheon, G.R. Rossman, G.J. Wasserburg, Mantle derived fluids in diamond micro inclusions, Nature 335 (1988) 84–789.
[3] G. Turner, R. Burgess, M. Bannon, Volatile-rich mantle fluids inferred from inclusions from diamond and mantle xenoliths, Nature 334 (1990) 653–655.
[4] M. Ozima, S. Zashu, Noble gas state of the ancient mantle as deduced from noble gases in coated diamonds, Earth Planet. Sci. Lett. 105 (1991) 13–27.
[5] N. Wada, J.-I. Matsuda, A noble gas study of cubic diamonds from Zaire: constraints on their mantle source, Geochim. Cosmochim. Acta 62 (1998) 2335–2344.
[6] R. Burgess, L.H. Johnson, D.P. Mattey, J.W. Harris, G. Turner, He, Ar and C isotopes in coated and polycrystalline diamonds, Chem. Geol. 146 (1998) 205–217.
[7] M. Schrauder, O. Navon, Hydrous and carbonatitic mantle fluids in fibrous diamonds from Jwaneng, Botswana, Geochim. Cosmochim. Acta 58 (1994) 761–771.
[8] E.S. Izraeli, J.W. Harris, O. Navon, Brine inclusions in diamonds: a new upper mantle fluid, Earth Planet. Sci. Lett. 187 (2001) 323–332.
[9] A.R. Lang, J.C. Walmsley, Apatite inclusion in natural diamond coat, Phys. Chem. Mineral. 9 (1983) 6–8.
[10] G.D. Guthrie, D.R. Veblen, O. Navon, G.R. Rossman, Submicrometer fluid inclusions in turbid-diamond coats, Earth Planet. Sci. Lett. 105 (1991) 1–12.

[11] J.C. Walmsley, A.R. Lang, Orientated biotite inclusions in diamond coat, Min. Mag. 56 (1992) 108–111.

[12] J.C. Walmsley, A.R. Lang, On sub-micrometer inclusions in diamond coat: crystallography and composition of ankerites and related carbonates, Min. Mag. 56 (1992) 533–543.

[13] T. Akagi, A. Masuda, Isotopic and elemental evidence for a relationship between kimberlite and Zaire cubic diamonds, Nature 336 (1988) 665–667.

[14] M. Ozima, S. Zashu, Y. Takigami, G. Turner, Origin of the anomalous ^{40}Ar-^{39}Ar age of Zaire cubic diamonds excess ^{40}Ar in pristine mantle fluids, Nature 337 (1989) 226–229.

[15] S.R. Boyd, D.P. Mattey, C.T. Pillinger, H.J. Milledge, M. Mendelssohn, M. Seal, Multiple growth events during diamond genesis: an integrated study of carbon and nitrogen isotopes and nitrogen aggregation state in coated stones, Earth Planet. Sci. Lett. 86 (1987) 341–353.

[16] M. Schrauder, C. Koeberl, O. Navon, Trace element analyses of fluid-bearing diamonds from Jwaneng, Botswana, Geochim. Cosmochim. Acta 60 (1996) 4711–4724.

[17] R. Burgess, G. Turner, Halogen geochemistry of mantle fluids in diamond, in: K.A. Farley (Ed.), Volatiles in the Earth and Solar system, Proc. AIP Conf. vol. 341, 1995, pp. 91–98.

[18] L.H. Johnson, R. Burgess, G. Turner, H.J. Milledge, J.W. Harris, Noble gas and halogen geochemistry of mantle fluids: comparison of African and Canadian diamonds, Geochim. Cosmochim. Acta 64 (2000) 717–732.

[19] J.G. Schilling, M.B. Bergeron, R. Evans, Halogens in the mantle beneath the North Atlantic, Philos. Trans. R. Soc. Lond. A 297 (1980) 147–178.

[20] B. Déruelle, G. Dreibus, A. Jambon, Iodine abundances in oceanic basalts: implications for Earth dynamics, Earth Planet. Sci. Lett. 108 (1992) 217–227.

[21] A. Jambon, B. Déruelle, G. Dreibus, F. Pineau, Chlorine and bromine abundance in MORB: the contrasting behaviour of the Mid-Atlantic Ridge and East Pacific Rise and implications for the chlorine geodynamic cycle, Chem. Geol. 126 (1995) 101–117.

[22] B. Villemant, G. Boudon, H_2O and halogen (F, Cl, Br) behaviour during shallow magma degassing processes, Earth Planet. Sci. Lett. 168 (1999) 271–286.

[23] W.L. Griffin, C.G. Ryan, F.V. Kaminsky, S.Y. O'Reilly, L.M. Natapov, T.T. Win, P.D. Kinny, I.P. Ilupin, The Siberian lithosphere traverse mantle terranes and the assembly of the Siberian craton, Tectonophysics 310 (1999) 1–35.

[24] D.G. Pearson, G. Bulanova, S. Shirey, R. Carlson, J. Milledge, Y. Barashkov, Re-Os isotope constraints on the age of Siberian diamonds, J. Conf. Abstr. 5 (2000) 776.

[25] D.G. Pearson, S.B. Shirey, G.P. Bulanova, R.W. Carlson, H.J. Milledge, Re-Os isotope measurements of single sulfide inclusions in a Siberian diamond and its nitrogen aggregation systematics, Geochim. Cosmochim. Acta 63 (1999) 703–711.

[26] S.H. Richardson, J.W. Harris, Antiquity of peridotitic diamonds from the Siberian craton, Earth Planet. Sci. Lett. 151 (1997) 271–277.

[27] R. Burgess, G. Turner, J.W. Harris, ^{40}Ar-^{39}Ar laser probe studies of clinopyroxene inclusions in eclogitic diamonds, Geochim. Cosmochim. Acta 56 (1992) 389–402.

[28] S.R. Boyd, C.T. Pillinger, H.J. Milledge, M.J. Mendelssohn, M. Seal, C and N isotopic composition and the infrared absorption spectra of coated diamonds: evidence for the regional uniformity of CO_2-H_2O rich fluids in the lithospheric mantle, Earth Planet. Sci. Lett. 109 (1992) 633–644.

[29] H. Craig, J. Lupton, Primordial neon, helium and hydrogen in oceanic basalts, Earth Planet. Sci. Lett. 31 (1976) 369–385.

[30] M.D. Kurz, W.J. Jenkins, S.R. Hart, Helium isotope systematics of oceanic islands and mantle heterogeneity, Nature 297 (1982) 43–47.

[31] P. Sarda, Th. Staudacher, C.J. Allègre, $^{40}Ar/^{36}Ar$ in MORB glasses: constraints on atmosphere and mantle evolution, Earth Planet. Sci. Lett. 72 (1985) 357–375.

[32] J.G. Schilling, C.K. Unni, M.L. Bender, Origin of chlorine and bromine in the oceans, Nature 273 (1978) 631–636.

[33] Y. Muramatsu, K.H. Wedepohl, The distribution of iodine in the Earth's crust, Chem. Geol. 147 (1998) 201–216.

[34] C. Allègre, G. Manhès, E. Lewin, Chemical composition of the Earth and the volatility control on planetary genetics, Earth Planet. Sci. Lett. 185 (2001) 49–69.

[35] S.A. Wilde, J.W. Valley, W.H. Peck, C.G. Graham, Evidence from detrital zircons for the existence of continental crust and oceans in the Earth 4.4 Gyr ago, Nature 409 (2001) 175–178.

[36] G. Dreibus, B. Spettel, H. Wänke, Halogens in meteorites and their primordial abundances, in: L.H. Ahrens (Ed.), Origin and Distribution of the Elements, Pergamon, Oxford, 1979, pp. 33–38.